Korean J. Chem. Eng., 33(5), 1728-1735 (2016)
DOI: 10.1007/s11814-016-0010-0

pISSN: 0256-1115
eISSN: 1975-7220

Structural identification of $DClO_4$ clathrate hydrates: Neutron powder diffraction analysis

Kyuchul Shin*,†, Minjun Cha, Wonhee Lee***, and Huen Lee****,†**

*School of Applied Chemical Engineering, Major in Applied Chemistry, Kyungpook National University, 80 Daehak-ro, Buk-gu, Daegu 41566, Korea
**Department of Energy and Resources Engineering, Kangwon National University, 1 Kangwondaehak-gil, Chuncheon-si, Gangwon-do 24341, Korea
***Climate Change Research Division, Korea Institute of Energy Research (KIER), Daejeon 34128, Korea
****Department of Chemical and Biomolecular Engineering, Korea Advanced Institute of Science and Technology (KAIST), 291 Daehak-ro, Yuseong-gu, Daejeon 34143, Korea
(*Received 22 November 2015 • accepted 7 January 2016*)

Abstract−Acid clathrate hydrates which do not contain hydrogen fluoride impurities are believed to include several vacancy sites in the host lattice for protonation of the framework. In this work, the crystal structures of a $DClO_4 \cdot 5.5D_2O$ solid at various temperatures were identified by the direct space method and Rietveld refinement of the neutron powder diffraction patterns. A position change of vacancy sites accompanying the shift of ClO_4^- guest ions in the $5^{12}6^2$ cavity toward the center of the cavity from the edge of the hexagonal face was observed at about 180 K, and this phenomenon is expected to result in weakened host proton-guest anion interactions and to induce a phase transition related to the proton conduction behavior of the $DClO_4$ clathrate. The present findings explain the proton dynamics of the hydrogen fluoride-free acid clathrate hydrates and provide a better understanding of the nature of guest-host interactions occurring on ion-doped hydrate materials.

Keywords: Clathrate, Hydrate, Neutron Powder Diffraction

INTRODUCTION

Clathrate hydrates are nonstoichiometric crystalline solids containing some interactions between the guest molecules or ions and the hydrogen-bonded water host framework [1,2]. Classical clathrate hydrates, which do not include any ionic species, are stabilized by van der Waals interaction only, while ionic clathrate hydrates show an ionic interaction between hydrophobic cationic or anionic guests and counterion-doped host cavities [2]. Because a proton or hydroxide ion doped in the host framework can substantially promote the ionic conductivity, some ionic clathrate hydrates have been recognized as possible solid electrolytes for gas sensors or supercapacitors [3-8].

A few strong acids have been reported to form clathrate structures in which anions are encaged into the protonated water framework [9-11]. There are two widely known crystal structures of acid clathrate hydrates. The first is a cubic *Im-3m* structure, also termed structure VII (sVII) by Jeffrey [1], comprising $4^6 6^8$ cavities only. Hexahydrates of HPF_6, $HAsF_6$, or $HSbF_6$ are the examples of this type. For these three hydrates, it was reported that a more correct composition of the framework is $H_3O^+ \cdot HF \cdot 4H_2O$ per one anion guest, instead of $6H_2O$ [9,10]. These hydrates have potential as a solid electrolyte because of their relatively high thermodynamic stability (higher melting point than room temperature) and high ionic conductivity [4].

Another type of acid clathrate hydrates is a cubic *Pm-3n* structure, also termed structure I (sI) by Jeffrey [1], comprising six $5^{12}6^2$ and two 5^{12} cavities with 46 H_2Os in a unit cell. $HPF_6 \cdot 7.67H_2O$, $HBF_4 \cdot 5.75H_2O$, and $HClO_4 \cdot 5.5H_2O$ are classified into this type. These hydrates have relatively low melting points (roughly lower than −40 °C), in contrast to the sVII type [11]. In particular, HPF_6 hydrate shows a structural transformation from thermodynamically stable sVII to less stable sI clathrate, caused by a slight increase of the hydration number [4]. The PF_6^- in sI hydrate occupies large $5^{12}6^2$ cavities only and small cavities remain vacant. On the other hand, smaller BF_4^- occupies both $5^{12}6^2$ and 5^{12} cavities, and thus the hydration number is approximately 5.75 (46 over 8). ClO_4^-, which has ionic size between those of PF_6^- and BF_4^-, also occupies both $5^{12}6^2$ and 5^{12} cavities; however, an O atom of ClO_4^- in the small 5^{12} cavity substitutes a host water molecule. This leads to a slightly reduced hydration number of $HClO_4$ clathrate, that is, approximately 5.5 (44 over 8) [11]. It is believed that protonation of the host lattice in HBF_4 and $HClO_4$ hydrates, which are HF-free clathrates, is achieved from several vacancies caused by replacing water molecules of the host with the F or O atoms of anion guests [11-14]. The vacancies existing in the host framework increase the degree of disorder in the crystal structure of these materials, and have caused unsatisfactory solutions in related structural analyses.

†To whom correspondence should be addressed.
E-mail: h_lee@kaist.ac.kr, kyuchul.shin@knu.ac.kr
‡This article is dedicated to Prof. Huen Lee on the occasion of his retirement from KAIST.

We report here the structural identification of $DClO_4 \cdot 5.5D_2O$ clathrate using the direct space method [15] and a Rietveld refinement analysis of the neutron powder diffraction (NPD) patterns. The neutron diffraction technique has the advantage of identifying light atoms such as deuterium because the neutrons interact with nuclei, while the X-ray diffraction technique interacting with electron clouds shows low sensitivity to light atoms. The atomic positions of ClO_4^-s in the $5^{12}6^2$ and 5^{12} cavities were determined by the direct space method, and the crystal structures at a range of temperatures from 30 K to 210 K were finally determined by the Rietveld refinement of NPD patterns. The distances between the O atoms of ClO_4^- and the host water oxygen were also calculated from the obtained solutions, in order to suggest the position of replaced water molecules for vacancies of the framework.

EXPERIMENTAL DETAILS

The NPD patterns of $DClO_4 \cdot 5.5D_2O$ were obtained from a previous study by the authors [16]. The previous work only focused on the determination of lattice parameters depending on the temperature without consideration of the detailed crystal structures (details of experimental procedures and discussion are explained in the reference). In this work, the structural identification of $DClO_4 \cdot 5.5D_2O$ was performed by the following procedure.

The ClO_4^- positions in the $5^{12}6^2$ and 5^{12} cavities were first determined by the direct space methods using the program FOX [17,18]. With the obtained initial guest coordinates, the NPD patterns were refined by the Rietveld method with the FULLPROF program [19]. During the analysis, ClO_4^- was assumed as a rigid body with identical isotropic thermal factors (B values) for all atoms. Soft distance constraints for the host D_2O (O-D covalent bond length: 0.98 Å and O···D hydrogen bond length: 1.74 Å) were applied and the site occupancies of all host and guest atoms were fixed. After the refinement, distances between the O atom of ClO_4^- in the 5^{12} cavity and host O atoms were calculated and the closest host O from the guest anion was determined to be a vacancy site. With the consideration of vacancies, the site occupancies of host atoms were modified and the structural refinement was then finalized.

RESULTS AND DISCUSSION

Fig. 1 shows the refined patterns of the $DClO_4 \cdot 5.5D_2O$ recorded at 30 K. The patterns recorded at 60, 90, 120, 150, 180, and 210 K were also refined with reasonable reliability factors. As reported previously, $DClO_4 \cdot 5.5D_2O$ has a cubic *Pm-3n* structure with lattice parameters of ~12 Å [1,11]. Temperature-dependent lattice parameters are shown in Fig. 2, and the atomic coordinates, the B values, and the site occupancies for each temperature are given in Tables 1 to 7. Significantly large B values of O and D atoms of the host framework in Tables 1 to 7 indicate that the crystal structure of $DClO_4 \cdot 5.5D_2O$ is highly disordered.

A previous study reported that the O atoms of ClO_4^-s occupy some vacant sites of the host framework [11]. In this study, the O-O distances between ClO_4^- and host oxygens were calculated from the refinement results and are shown in Fig. 3. There are three crystallographically distinct O atom sites in the sI host framework,

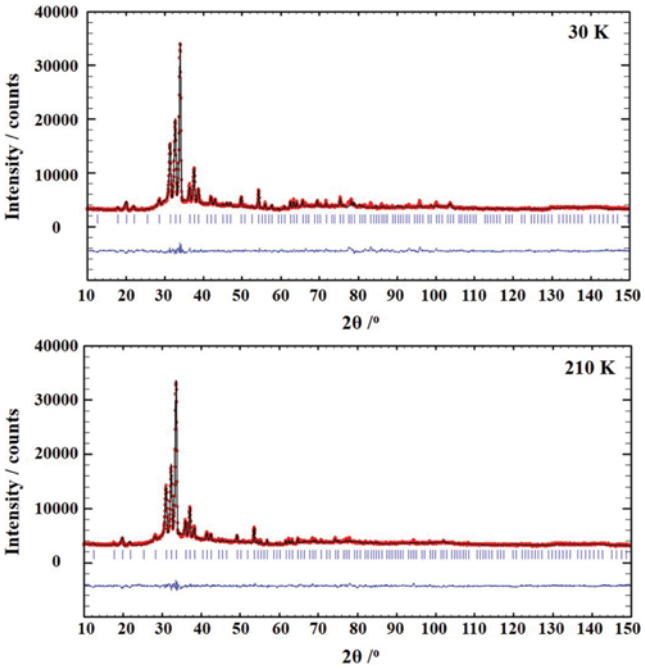

Fig. 1. The refined NPD patterns of $DClO_4 \cdot 5.5D_2O$ recorded at 30 K and 210 K by Rietveld analysis with the direct space method. Tick marks indicate the Bragg positions for the cubic *Pm-3n*, and the lines below zero intensity indicate the differences between the observed and the calculated patterns.

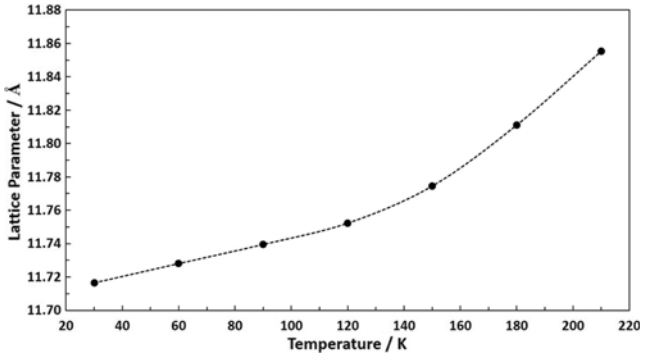

Fig. 2. The lattice parameters of $DClO_4 \cdot 5.5D_2O$ calculated from this work.

denoted by Wyckoff symbols with the number of sites in the unit cell, *k*(24), *i*(16), and *c*(6), respectively. The 5^{12} cavities comprise the oxygens of *k*- and *i*-sites while the $5^{12}6^2$ cavities comprise the oxygens of *k*-, *i*-, and *c*-sites. As shown in Fig. 3, the closest O atom site of the host lattice to ClO_4^- in the 5^{12} cavity is O_k with O_S-O_k distances of 1.6-1.8 Å at a range of temperatures from 30 K to 150 K, and thus the most probable site for vacancies in the host might be the *k*-site at low temperature. This resembles the case of a methanol guest in the sII THF hydrate, where the O atom of methanol is 1.83 Å apart from a water O atom [20]. Under those short O-O distance conditions, a host O atom is absent and the guest O atom is connected to the three neighboring water O atoms by hydrogen bonding. The O_S-O_i distances in the $DClO_4 \cdot 5.5D_2O$ are around 2.0-2.3 Å (Fig. 3), implying hydrogen bonding between two O atoms,

Table 1. Atomic coordinates and isotropic temperature factors for $DClO_4 \cdot 5.5D_2O$ at 30 K. Space group: *Pm-3n*, Lattice parameter: a= 11.7165(12) Å, Reliability factors: χ^2=4.78 and R_{wp}=16.1% (background subtracted). D_{ck}: deuterium covalently connecting with O_c and hydrogen bonding with O_k (O_c-D_{ck}···O_k)

Atom	x	y	z	B (Å^2)	g	Site
O_i	0.1826(3)	0.1826	0.1826	14.1(4)	1	16*i*
O_k	0	0.3073(5)	0.1301(5)	12.0(4)	0.9167	24*k*
O_c	0	0.5	0.25	7.6(3)	1	6*c*
D_{ii}	0.2315(3)	0.2315	0.2315	3.5(3)	0.5	16*i*
D_{ck}	0	0.4473(11)	0.1831(14)	34.8(10)	0.5	24*k*
D_{kc}	0	0.3800(8)	0.1709(10)	7.9(4)	0.4583	24*k*
D_{kk}	0	0.3370(10)	0.0532(6)	5.0(3)	0.4583	24*k*
D_{ki}	0.0746(7)	0.2707(10)	0.1320(11)	14.0(6)	0.4583	48*l*
D_{ik}	0.1171(8)	0.2340(9)	0.1747(10)	13.6(5)	0.5	48*l*
Cl_L	0.2821	0.5429	0.9969	1.2(1)	0.125	48*l*
O_L1	0.3841	0.5325	1.0705	1.2	0.125	48*l*
O_L2	0.2827	0.6556	0.9398	1.2	0.125	48*l*
O_L3	0.1780	0.5322	1.0675	1.2	0.125	48*l*
O_L4	0.2835	0.4516	0.9097	1.2	0.125	48*l*
Cl_S	0.9333	0.9528	0.9977	0.01	0.0417	48*l*
O_S1	1.0005	0.8634	0.9390	0.01	0.0417	48*l*
O_S2	0.9957	0.9919	1.1002	0.01	0.0417	48*l*
O_S3	0.8214	0.9055	1.0320	0.01	0.0417	48*l*
O_S4	0.9155	1.0502	0.9194	0.01	0.0417	48*l*

Table 2. Atomic coordinates and isotropic temperature factors for $DClO_4 \cdot 5.5D_2O$ at 60 K. Space group: *Pm-3n*, Lattice parameter: a= 11.7281(12) Å, Reliability factors: χ^2=4.37 and R_{wp}=16.2% (background subtracted)

Atom	x	y	z	B (Å^2)	g	Site
O_i	0.1828(3)	0.1828	0.1828	17.1(6)	1	16*i*
O_k	0	0.3066(5)	0.1250(5)	12.7(4)	0.9167	24*k*
O_c	0	0.5	0.25	6.4(3)	1	6*c*
D_{ii}	0.2325(3)	0.2325	0.2325	2.8(2)	0.5	16*i*
D_{ck}	0	0.4437(12)	0.1853(15)	33.0(10)	0.5	24*k*
D_{kc}	0	0.3699(11)	0.1815(13)	10.1(5)	0.4583	24*k*
D_{kk}	0	0.3559(9)	0.0576(7)	7.7(4)	0.4583	24*k*
D_{ki}	0.0754(6)	0.2689(8)	0.1224(9)	11.2(4)	0.4583	48*l*
D_{ik}	0.1114(6)	0.2290(6)	0.1792(8)	8.9(3)	0.5	48*l*
Cl_L	0.4940	0.0496	0.2202	0.93(2)	0.125	48*l*
O_L1	0.5653	0.0529	0.3242	0.93	0.125	48*l*
O_L2	0.4271	0.1562	0.2117	0.93	0.125	48*l*
O_L3	0.4155	−0.0489	0.2262	0.93	0.125	48*l*
O_L4	0.5681	0.0383	0.1188	0.93	0.125	48*l*
Cl_S	0.0398	0.9929	0.9252	0.87(45)	0.0417	48*l*
O_S1	0.0331	1.0458	0.8109	0.87	0.0417	48*l*
O_S2	0.0201	1.0809	1.0134	0.87	0.0417	48*l*
O_S3	0.1541	0.9421	0.9414	0.87	0.0417	48*l*
O_S4	−0.0480	0.9029	0.9351	0.87	0.0417	48*l*

at the same range of temperature. In the case of the $5^{12}6^2$ cavities, the distances are 2.2-2.3 Å for O_L-O_k, 2.6-2.7 Å for O_L-O_i, and 2.8-2.9 Å for O_L-O_c, respectively. The ClO_4^- in the large $5^{12}6^2$ cavity also prefers the space near the vacancies at these temperatures.

An interesting feature is observed over 150 K. At 180 K and 210 K (Fig. 3), the closest host O site changes from O_k to O_i, (O_S-O_i distances: 1.88 Å at 180 K and 1.55 Å at 210 K), reflecting that the vacancy site moves. In the $5^{12}6^2$ cavities, the O_L-O_i distance retains a similar value (2.54 Å) to those below 180 K, while the O_L-O_k and the O_L-O_c distances increase up to 2.56 Å and 3.27 Å, respectively.

Table 3. Atomic coordinates and isotropic temperature factors for $DClO_4$·5.5D_2O at 90 K. Space group: *Pm-3n*, Lattice parameter: a= 11.7395(14) Å, Reliability factors: χ^2=4.48 and R_{wp}=16.6% (background subtracted)

Atom	x	y	z	B (Å^2)	g	site
O_i	0.1828(3)	0.1828	0.1828	18.7(6)	1	16*i*
O_k	0	0.3068(5)	0.1231(5)	12.5(4)	0.9167	24*k*
O_c	0	0.5	0.25	6.5(3)	1	6*c*
D_{ii}	0.2324(3)	0.2324	0.2324	3.3(3)	0.5	16*i*
D_{ck}	0	0.4424(12)	0.1863(15)	30.6(10)	0.5	24*k*
D_{kc}	0	0.3663(11)	0.1845(13)	9.8(5)	0.4583	24*k*
D_{kk}	0	0.3597(9)	0.0589(8)	9.3(4)	0.4583	24*k*
D_{ki}	0.0761(6)	0.2699(8)	0.1182(9)	12.0(5)	0.4583	48*l*
D_{ik}	0.1104(6)	0.2294(6)	0.1821(8)	7.8(3)	0.5	48*l*
Cl_L	0.5059	0.9498	0.2212	0.65(14)	0.125	48*l*
O_L1	0.5836	1.0487	0.2286	0.65	0.125	48*l*
O_L2	0.4325	0.9614	0.1195	0.65	0.125	48*l*
O_L3	0.4339	0.9451	0.3246	0.65	0.125	48*l*
O_L4	0.5735	0.8438	0.2124	0.65	0.125	48*l*
Cl_S	0.0036	0.0725	0.0469	0.82(52)	0.0417	48*l*
O_S1	0.0666	0.1808	0.0605	0.82	0.0417	48*l*
O_S2	−0.0521	0.0423	0.1558	0.82	0.0417	48*l*
O_S3	0.0840	−0.0189	0.0141	0.82	0.0417	48*l*
O_S4	−0.0838	0.0858	−0.0428	0.82	0.0417	48*l*

Table 4. Atomic coordinates and isotropic temperature factors for $DClO_4$·5.5D_2O at 120 K. Space group: *Pm-3n*, Lattice parameter: a= 11.7523(12) Å, Reliability factors: χ^2=3.68 and R_{wp}=15.2% (background subtracted)

Atom	x	y	z	B (Å^2)	g	Site
O_i	0.1828(3)	0.1828	0.1828	17.2(6)	1	16*i*
O_k	0	0.3046(5)	0.1282(5)	9.4(3)	0.9167	24*k*
O_c	0	0.5	0.25	5.8(3)	1	6*c*
D_{ii}	0.2313(3)	0.2313(3)	0.2313(3)	3.8(3)	0.5	16*i*
D_{ck}	0	0.4466(11)	0.1818(13)	33.4(10)	0.5	24*k*
D_{kc}	0	0.3748(8)	0.1743(9)	6.0(3)	0.4583	24*k*
D_{kk}	0	0.3442(10)	0.0537(7)	8.0(4)	0.4583	24*k*
D_{ki}	0.0744(7)	0.2692(10)	0.1271(12)	20.5(9)	0.4583	48*l*
D_{ik}	0.1159(6)	0.2340(7)	0.1789(9)	11.0(3)	0.5	48*l*
Cl_L	0.5074	0.9508	0.2215	0.65(13)	0.125	48*l*
O_L1	0.5875	0.9618	0.1250	0.65	0.125	48*l*
O_L2	0.4239	1.0449	0.2175	0.65	0.125	48*l*
O_L3	0.5713	0.9560	0.3298	0.65	0.125	48*l*
O_L4	0.4470	0.8407	0.2136	0.65	0.125	48*l*
Cl_S	0.9978	0.0445	0.0688	0.81(50)	0.0417	48*l*
O_S1	1.0099	0.1511	0.1346	0.81	0.0417	48*l*
O_S2	0.8791	0.0332	0.0286	0.81	0.0417	48*l*
O_S3	1.0268	−0.0536	0.1421	0.81	0.0417	48*l*
O_S4	1.0755	0.0473	−0.0302	0.81	0.0417	48*l*

This indicates that the ClO_4^- in the large cavity becomes less off-centered and more disordered at temperature higher than 180 K. The thermal factors (the B values), which are related to the degree of atom vibration, also show extraordinary trends at around 180 K. Figs. 4, 5, and 6 exhibit the B values of guest anions and host atoms. Except for the cases of O_k and D_{ik} only, all the B values show a rapid increment at 180 K, and then decrease back to the values of low temperatures at 210 K (Figs. 4, 5, and 6).

The crystal information of $DClO_4$·5.5D_2O obtained from this work implies that there should be a phase transition at around 180 K. In a previously reported study on the proton dynamics in $HClO_4$·5.5H_2O [12] the electrical conductivity of $HClO_4$ hydrate decreased

Table 5. Atomic coordinates and isotropic temperature factors for $DClO_4 \cdot 5.5D_2O$ at 150 K. Space group: *Pm-3n*, Lattice parameter: a= 11.7745(13) Å, Reliability factors: χ^2=3.53 and R_{wp}=15.1% (background subtracted)

Atom	x	y	z	B (Å^2)	g	Site
O_i	0.1833(3)	0.1833	0.1833	16.1(5)	1	16*i*
O_k	0	0.3059(5)	0.1262(5)	9.8(3)	0.9167	24*k*
O_c	0	0.5	0.25	4.2(2)	1	6*c*
D_{ii}	0.2319(3)	0.2319(3)	0.2319(3)	3.9(3)	0.5	16*i*
D_{ck}	0	0.4457(11)	0.1837(13)	34.0(10)	0.5	24*k*
D_{kc}	0	0.3746(9)	0.1753(10)	7.3(4)	0.4583	24*k*
D_{kk}	0	0.3494(10)	0.0537(8)	9.5(4)	0.4583	24*k*
D_{ki}	0.0770(7)	0.2726(9)	0.1306(11)	14.9(7)	0.4583	48*l*
D_{ik}	0.1118(7)	0.2254(8)	0.1774(10)	11.8(4)	0.5	48*l*
Cl_L	0.0480	0.7789	0.4925	0.42(12)	0.125	48*l*
O_L1	0.0409	0.8763	0.4135	0.42	0.125	48*l*
O_L2	−0.0468	0.7849	0.5749	0.42	0.125	48*l*
O_L3	0.1574	0.7829	0.5542	0.42	0.125	48*l*
O_L4	0.0404	0.6716	0.4276	0.42	0.125	48*l*
Cl_S	0.9529	0.0533	0.9629	3.0(6)	0.0417	48*l*
O_S1	0.9826	0.1700	0.9270	3.0	0.0417	48*l*
O_S2	0.8307	0.0481	0.9915	3.0	0.0417	48*l*
O_S3	1.0208	0.0219	1.0638	3.0	0.0417	48*l*
O_S4	0.9774	-0.0268	0.8693	3.0	0.0417	48*l*

Table 6. Atomic coordinates and isotropic temperature factors for $DClO_4 \cdot 5.5D_2O$ at 180 K. Space group: *Pm-3n*, Lattice parameter: a= 11.8110(13) Å, Reliability factors: χ^2=4.13 and R_{wp}=16.7% (background subtracted)

Atom	x	y	z	B (Å^2)	g	Site
O_i	0.1832(3)	0.1832	0.1832	23.0(8)	0.875	16*i*
O_k	0	0.3185(5)	0.1392(5)	16.1(4)	1	24*k*
O_c	0	0.5	0.25	12.9(5)	1	6*c*
D_{ii}	0.2313(3)	0.2313(3)	0.2313(3)	17.6(9)	0.4375	16*i*
D_{ck}	0	0.4625(10)	0.1740(10)	51.7(10)	0.5	24*k*
D_{kc}	0	0.4020(8)	0.1379(12)	68.4(10)	0.5	24*k*
D_{kk}	0	0.3050(17)	0.0539(8)	27.4(9)	0.5	24*k*
D_{ki}	0.0657(14)	0.2667(16)	0.1479(18)	49.7(10)	0.5	48*l*
D_{ik}	0.1140(6)	0.2326(6)	0.1872(7)	6.2(2)	0.4375	48*l*
Cl_L	0.9578	0.7921	0.5423	3.2(2)	0.125	48*l*
O_L1	0.8912	0.7197	0.6198	3.2	0.125	48*l*
O_L2	1.0598	0.7300	0.5045	3.2	0.125	48*l*
O_L3	0.9923	0.8966	0.6021	3.2	0.125	48*l*
O_L4	0.8879	0.8221	0.4428	3.2	0.125	48*l*
Cl_S	0.9589	0.9575	0.9557	7.7(8)	0.0417	48*l*
O_S1	1.0514	0.8767	0.9807	7.7	0.0417	48*l*
O_S2	0.9806	1.0129	0.8456	7.7	0.0417	48*l*
O_S3	0.9538	1.0443	1.0459	7.7	0.0417	48*l*
O_S4	0.8500	0.8959	0.9508	7.7	0.0417	48*l*

to very weak values below 170 K and the activation energy changed from 0.29 eV for over 180 K to 0.37 eV for below 180 K. The deuterium quadrupole spectrum of $HClO_4 \cdot 5.5D_2O$ also showed the characteristic shape of immobilized deuterons in a temperature range below ~170 K. In another previous study [13] the measurement of "fixed-window scan (FWS)," that is, the collection of neutrons that are elastically scattered only, showed a slope change of the FWS intensity curve at approximately 170 K, implying a change of proton dynamics at this temperature. Therefore, the drastic changes observed at ~180 K in this study are due to the phase transition from a "frozen" (i.e., the reorientation of water molecules is difficult to occur) to a "relaxed" (i.e., the reorientation easily possible) host frame-

Table 7. Atomic coordinates and isotropic temperature factors for $DClO_4 \cdot 5.5D_2O$ at 210 K. Space group: *Pm-3n*, Lattice parameter: a= 11.8553(21) Å, Reliability factors: χ^2=3.58 and R_{wp}=15.3% (background subtracted)

Atom	x	y	z	B (Å^2)	g	Site
O_i	0.1841(3)	0.1841	0.1841	9.5(3)	0.875	16*i*
O_k	0	0.3090(6)	0.1356(5)	19.4(6)	1	24*k*
O_c	0	0.5	0.25	11.3(6)	1	6*c*
D_{ii}	0.2317(3)	0.2317(3)	0.2317(3)	5.5(5)	0.4375	16*i*
D_{ck}	0	0.4208(11)	0.2314(19)	36.7(10)	0.5	24*k*
D_{kc}	0	0.3938(6)	0.1504(10)	8.4(4)	0.5	24*k*
D_{kk}	0	0.3255(10)	0.0561(6)	6.2(3)	0.5	24*k*
D_{ki}	0.0687(8)	0.2596(9)	0.1367(11)	13.8(6)	0.5	48*l*
D_{ik}	0.1278(12)	0.2402(12)	0.1721(17)	14.4(7)	0.4375	48*l*
Cl_L	0.9581	0.2212	0.5128	2.2(2)	0.125	48*l*
O_L1	0.9474	0.2117	0.3888	2.2	0.125	48*l*
O_L2	0.9947	0.1116	0.5599	2.2	0.125	48*l*
O_L3	0.8477	0.2527	0.5617	2.2	0.125	48*l*
O_L4	1.0424	0.3088	0.5407	2.2	0.125	48*l*
Cl_S	0.0383	0.0533	0.9604	1.7(6)	0.0417	48*l*
O_S1	−0.0129	0.1103	1.0589	1.7	0.0417	48*l*
O_S2	−0.0467	0.0429	0.8696	1.7	0.0417	48*l*
O_S3	0.0776	−0.0603	0.9938	1.7	0.0417	48*l*
O_S4	0.1351	0.1204	0.9191	1.7	0.0417	48*l*

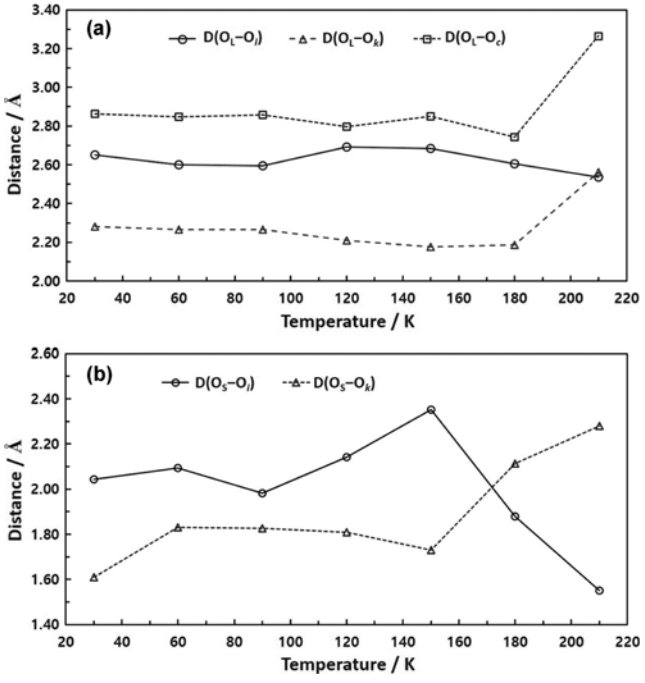

Fig. 3. The shortest O-O distances between guest ClO_4^- ions and host water molecules (a) in the $5^{12}6^2$ cavity and (b) in the 5^{12} cavity.

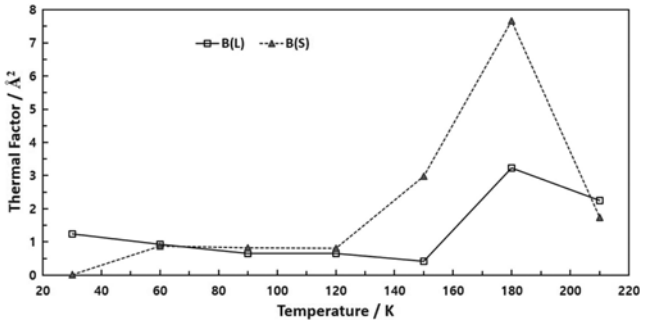

Fig. 4. The isotropic thermal factors of guest ions in the $5^{12}6^2$ cavity (B(L)) and in the 5^{12} cavity (B(S)).

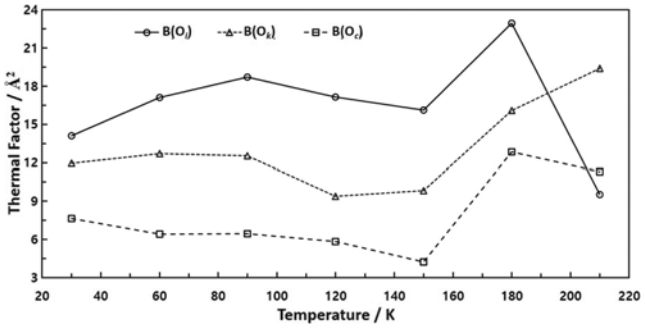

Fig. 5. The isotropic thermal factors of host oxygens.

work, which is capable of conducting protons.

As shown in Fig. 3, the phase transition occurring in the $DClO_4 \cdot 5.5D_2O$ at ~180 K is accompanied by the shift of the vacancy sites in the host lattice. At 30 K-150 K, the closest host O site from the O atoms of ClO_4^-s in both 5^{12} and $5^{12}6^2$ cavities is O_k, which comprises hexagonal faces of the $5^{12}6^2$ cavities. In our previous study on the binary structure II (sII, cubic *Fd-3m*) clathrate hydrate of a strong base, tetramethylammonium hydroxide [21], we found that the proton hole due to the incorporation of OH^- in the hydrate

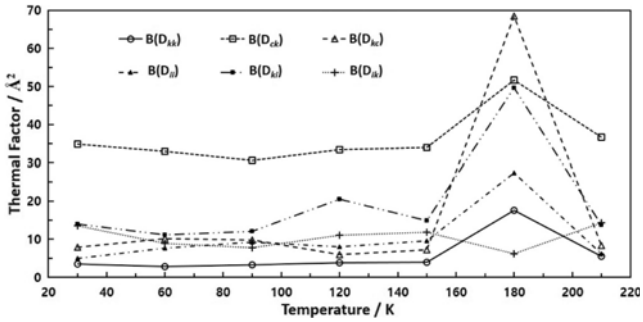

Fig. 6. The isotropic thermal factors of host deuteriums.

host is located at the hexagonal faces of the $5^{12}6^4$ cavity in the sII framework at low temperature, because the hydrogen bond in the hexagonal face is less stable than that in the pentagonal face [22]. Similarly, in the sI $DClO_4$ hydrate, the acidic proton from $DClO_4$ might be incorporated in the vacancy of the O_k site of the hexagonal face, and immobilized by strong interactions with both ClO_4^-s of the 5^{12} and the $5^{12}6^2$ cavities. The thermal factors of guest ions in both large and small cavities are quite low at this temperature region (Fig. 4). As temperature increases over 150 K, a phase transition occurs in the $DClO_4{\cdot}5.5D_2O$ clathrate structure. At 180 K, the vacancies start to move from O_k to O_i sites and the B values of the guest ions and host protons rapidly increase because the degree of disorder of the crystal in the transition state might be higher (Figs. 3 and 4). At 210 K, the vacancies completely move to O_i sites comprising the pentagonal faces only (Fig. 3), and the ClO_4^- in the large cavity moves toward the center of the cavity (the closest O-O distance between the host and ClO_4^- in the $5^{12}6^2$ cavity: 2.18 Å at 150 K and 2.54 Å at 210 K, respectively) because the O_i site in the $5^{12}6^2$ cavity is a geometrically less favorable position to interact with guest molecules than the O_k site (Fig. 7) [23]. Finally, the interactions between the incorporated protons and ClO_4^- ions weaken and the host framework become sufficiently "relaxed" to conduct protons.

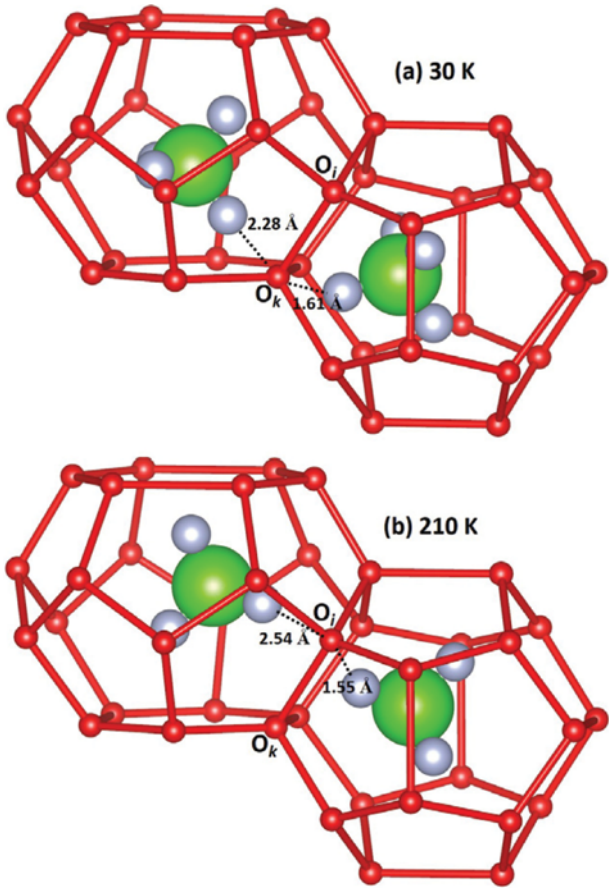

Fig. 7. Guest ions (ClO_4^-) in the large (left) and small (right) cavities at (a) 30 K and (b) 210 K. The dotted lines exhibit the shortest distances between host O atom and guest O atom for each cavity (Deuterium atoms in host are omitted).

CONCLUSION

We identified the crystal structures of the $DClO_4{\cdot}5.5D_2O$ and demonstrated that the phase transition related to the proton conductivity behavior of this ionic clathrate material appearing at about 180 K is accompanied by a shift of the vacancy site in the host framework. At low temperature, the vacancies were located at the hexagonal face of the $5^{12}6^2$ cavity, which is a position strongly interacting with both ClO_4^-s of the large and small cavities. Above the transition temperature, the vacancies move to the pentagonal face and the ClO_4^- in the large cavity also moves toward the center of cavity. Because the acid clathrate hydrates usually show higher proton conductivity than most hydroxide or halide clathrate hydrates [5], the crystal structures and proton conduction mechanisms of these materials should be fully understood to realize their use as practical solid electrolytes. The present work provides important information on the proton dynamics of acid clathrate hydrates containing vacancy sites in the host framework, and provides a better understanding for the nature of guest-host interactions and inclusion phenomena of ionic clathrate hydrates.

ACKNOWLEDGEMENTS

This research was supported by Kyungpook National University Research Fund, 2014.

REFERENCES

1. G. A. Jeffrey, in *Inclusion Compounds*, Vol. 1, pp. 135-190; J. L. Atwood, J. E. D. Davies and D. D. MacNicol Eds., Academic Press, London (1984).
2. K. Shin, J.-H. Cha, Y. Seo and H. Lee, *Chem. Asian J.*, **5**, 22 (2010).
3. S. Choi, K. Shin and H. Lee, *J. Phys. Chem. B*, **111**, 10224 (2007).
4. J.-H. Cha, K. Shin, S. Choi, S. Lee and H. Lee, *J. Phys. Chem. C*, **112**, 13332 (2008).
5. J.-H. Cha, W. Lee and H. Lee, *J. Mater. Chem.*, **19**, 6542 (2009).
6. W. Lee, D. Lim and H. Lee, *Electrochim. Acta*, **109**, 852 (2013).
7. J.-H. Cha, W. Lee and H. Lee, *Angew. Chem. Int. Ed.*, **48**, 8687 (2009).
8. W. Lee, M. Kown, S. Park, D. Lim, J.-H. Cha and H. Lee, *Chem. Asian J.*, **8**, 1569 (2013).

9. D. W. Davidson and S. K. Garg, *Can. J. Chem.*, **50**, 3515 (1972).
10. D. W. Davidson, L. D. Calvert, F. Lee and J. A. Ripmeester, *Inorg. Chem.*, **20**, 2013 (1981).
11. D. Mootz, E.-J. Oellers and M. Wiebcke, *J. Am. Chem. Soc.*, **109**, 1200 (1987).
12. T.-H. Huang, R. A. Davis, U. Frese and U. Stimming, *J. Phys. Chem.*, **92**, 6874 (1988).
13. A. Desmedt, F. Stallmach, R. E. Lechner, D. Cavagnat, J.-C. Lassègues, F. Guillaime, J. Grondin and M. A. Gonzalez, *J. Chem. Phys.*, **121**, 11916 (2004).
14. A. Desmedt, R. E. Lechner, J.-C. Lassegues, F. Guillaime, D. Cavagnat and J. Grondin, *Solid State Ionics*, **252**, 19 (2013).
15. S. Takeya, K. A. Udachin, I. L. Moudrakovski, R. Susilo and J. A. Ripmeester, *J. Am. Chem. Soc.*, **132**, 524 (2010).
16. K. Shin, W. Lee, M. Cha, D.-Y. Koh, Y. N. Choi, H. Lee, B. S. Son, S. Lee and H. Lee, *J. Phys. Chem. B*, **115**, 958 (2011).
17. F. Favre-Nicolin and R. Cerny, *J. Appl. Cryst.*, **35**, 734 (2002).
18. R. Cerny and F. Favre-Nicolin, *Z. Kristrallogr-Cryst. Mater.*, **222**, 105 (2007).
19. J. Rodriguez-Carvajal, *Phys. B*, **192**, 55 (1993).
20. K. Shin, K. A. Udachin, I. L. Moudrakovski, D. M. Leek, S. Alavi, C. I. Ratcliffe and J. A. Ripmeester, *Proc. Natl. Acad. Sci. USA*, **110**, 8437 (2013).
21. K. Shin, M. Cha, W. Lee, Y. Seo and H. Lee, *J. Phys. Chem. C*, **118**, 15193 (2014).
22. K. Shin, R. Kumar, K. A. Udachin, S. Alavi and J. A. Ripmeester, *Proc. Natl. Acad. Sci. USA*, **109**, 14785 (2012).
23. K. Momma and F. Izumi, *J. Appl. Crystallogr.*, **44**, 1272 (2011).